

4

Observations of Large-Amplitude, Whistler-Mode Wave Ducts in the Outer Plasmasphere

H. C. KOONS
Space Sciences Laboratory
Laboratory Operations
The Aerospace Corporation
El Segundo, CA 90245

12 February 1990

Prepared for

SPACE SYSTEMS DIVISION
AIR FORCE SYSTEMS COMMAND
Los Angeles Air Force Base
P.O. Box 92960
Los Angeles, CA 90009-2960

AD-A219 981

APPROVED FOR PUBLIC RELEASE;
DISTRIBUTION IS UNLIMITED

DTIC
ELECTE
APR 3 1990
S B D

This report was submitted by The Aerospace Corporation, El Segundo, CA 90245, under Contract No. F04701-88-C-0089 with the Space Systems Division, P.O. Box 92960, Los Angeles, CA 90009-2960. It was reviewed and approved for The Aerospace Corporation by H. R. Rugge, Director, Space Sciences Laboratory.

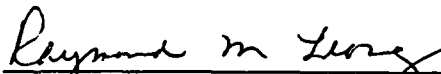
Lt Tyron Fisher was the project officer for the Mission-Oriented Investigation and Experimentation (MOIE) program.

This report has been reviewed by the Public Affairs Office (PAS) and is releasable to the National Technical Information Service (NTIS). At NTIS, it will be available to the general public, including foreign nationals.

This technical report has been reviewed and is approved for publication. Publication of this report does not constitute Air Force approval of the report's findings or conclusions. It is published only for the exchange and stimulation of ideas.



TYRON FISHER, LT, USAF
MOIE Project Officer
SSD/CLFPL



RAYMOND M. LEONG, MAJ, USAF
MOIE Program Manager
AFSTC/WCO OL-AB

UNCLASSIFIED

SECURITY CLASSIFICATION OF THIS PAGE

REPORT DOCUMENTATION PAGE				
1a. REPORT SECURITY CLASSIFICATION Unclassified		1b. RESTRICTIVE MARKINGS		
2a. SECURITY CLASSIFICATION AUTHORITY		3. DISTRIBUTION/AVAILABILITY OF REPORT Approved for public release; distribution unlimited.		
2b. DECLASSIFICATION/DOWNGRADING SCHEDULE		5. MONITORING ORGANIZATION REPORT NUMBER(S) SSD-TR-89-92		
4. PERFORMING ORGANIZATION REPORT NUMBER(S) TR-0089(4940-06)-5		7a. NAME OF MONITORING ORGANIZATION Space Systems Division		
6a. NAME OF PERFORMING ORGANIZATION The Aerospace Corporation Laboratory Operations		6b. OFFICE SYMBOL (If applicable)		7b. ADDRESS (City, State, and ZIP Code) Los Angeles Air Force Base Los Angeles, CA 90009-2960
6c. ADDRESS (City, State, and ZIP Code) El Segundo, CA 90245-4691		9. PROCUREMENT INSTRUMENT IDENTIFICATION NUMBER F04701-88-C-0089		
8a. NAME OF FUNDING/SPONSORING ORGANIZATION		8b. OFFICE SYMBOL (If applicable)		10. SOURCE OF FUNDING NUMBERS
8c. ADDRESS (City, State, and ZIP Code)		PROGRAM ELEMENT NO.	PROJECT NO.	TASK NO.
WORK UNIT ACCESSION NO.				
11. TITLE (Include Security Classification) Observations of Large-Amplitude, Whistler-Mode Wave Ducts in the Outer Plasmasphere				
12. PERSONAL AUTHOR(S) Koons, H. C.				
13a. TYPE OF REPORT		13b. TIME COVERED FROM _____ TO _____		14. DATE OF REPORT (Year, Month, Day) 1990 February 12
15. PAGE COUNT 23				
16. SUPPLEMENTARY NOTATION:				
17. COSATI CODES			18. SUBJECT TERMS (Continue on reverse if necessary and identify by block number)	
FIELD	GROUP	SUB-GROUP	Whistlers ; Wave ducts ; Plasmasphere.	
19. ABSTRACT (Continue on reverse if necessary and identify by block number)				
<p>Strong enhancements of whistler-mode hiss emissions have been observed to correlate with plasma density enhancements in the outer plasmasphere between $L = 4$ and $L = 6$ ($L =$ McIlwain's parameter). This indicates that these density enhancements are acting as whistler-mode wave ducts. The wave and density observations were made simultaneously by The Aerospace Corporation swept frequency receiver (SFR) aboard the Active Magnetospheric Particle Tracer Explorer (AMPTE) ion release module (IRM) spacecraft. The plasma density is determined from a narrowband line near the plasma frequency. The hiss emissions generally occur below 2 kHz. The ducts consist of density enhancements of more than 40%. Density gradients on the sides of the ducts range from 0.10 to 0.24 electrons per cubic centimeter per kilometer. The half width of each duct is typically 250 km. The wave intensity maximizes about 15 km from the center of the duct toward the outside, i.e., the side with a negative density gradient with increasing distance. The wave intensity near the center of a duct is an order of magnitude higher than the wave intensity at the density minimum between ducts.</p>				
20. DISTRIBUTION/AVAILABILITY OF ABSTRACT <input checked="" type="checkbox"/> UNCLASSIFIED/UNLIMITED <input type="checkbox"/> SAME AS RPT. <input type="checkbox"/> DTIC USERS			21. ABSTRACT SECURITY CLASSIFICATION Unclassified	
22a. NAME OF RESPONSIBLE INDIVIDUAL			22b. TELEPHONE (Include Area Code)	22c. OFFICE SYMBOL

PREFACE

I wish to thank G. Haerendel, the Principal Investigator for the AMPTE IRM spacecraft, of the Institut für Extraterrestrische Physik, Max-Planck-Institut für Physik und Astrophysik, for the opportunity to participate in the AMPTE program. It is a pleasure to acknowledge the efforts and stimulating discussions with the other members of the Plasma Wave team, D. A. Gurnett, R. Holzworth, J. L. Roeder, O. Bauer, R. Treumann, and the original Principal Investigator for the team, B. Häusler. I would especially like to thank D. J. Gorney for the formulas for the field line curvature calculation. The research at The Aerospace Corporation was supported in part by the Office of Naval Research and in part by the U. S. Air Force Systems Command, Space Systems Division, under Contract No. F04701-88-C-0089.

Accession For	
NTIS GRA&I	<input checked="checked" type="checkbox"/>
DTIC TAB	<input type="checkbox"/>
Unannounced	<input type="checkbox"/>
Justification	
By	
Distribution/	
Availability Codes	
Dist	Avail and/or Special
A-1	

CONTENTS

PREFACE.....	1
I. INTRODUCTION.....	7
II. DISCUSSION.....	9
A. Instrumentation.....	9
B. Density Measurements.....	9
C. Data.....	10
D. Whistler Ducting Criterion.....	21
III. SUMMARY.....	23
REFERENCES.....	25

TABLE

1.	Duct Parameters for the Density Enhancements Observed on January 12, 1986.....	18
----	--	----

FIGURES

1.	Spectrogram from the VLF/MF Swept Frequency Receiver on January 12, 1986.....	11
2.	Spectrogram from the VLF/MF Swept Frequency Receiver on September 23, 1985.....	13
3.	Electron Density and Whistler-Mode Wave Amplitude at 350 Hz on January 12, 1986.....	16
4.	Cross-Correlogram of the Electron Density and Whistler-Mode Wave Amplitude. January 12, 1986; September 23, 1985; December 24, 1984.....	19
5.	Electron Density and Whistler-Mode Wave Amplitude at 350 Hz on September 23, 1985.....	20
6.	Electron Density and Whistler-Mode Wave Amplitude at 350 Hz on December 24, 1984.....	22

I. INTRODUCTION

The propagation of whistler-mode waves from hemisphere to hemisphere in the plasmasphere is generally believed to occur in ionization ducts that are aligned with the geomagnetic field. The theory of ducting is well developed. Smith [1961] showed that waves can propagate from hemisphere to hemisphere in relatively modest (20%) density enhancements. Gorney and Thorne [1980] compared the ducting ability of both "bell-shaped" and "ledge-shaped" ducts and concluded that modest (again 20%) perturbations with either shape are capable of effective ducting in middle latitudes. Inan and Bell [1977] showed that the density gradient at the plasmopause is also an effective whistler-mode wave duct.

Observations by the Orbiting Geophysical Observatory satellite (OGO 1) provided the first in situ evidence for whistler ducts [Smith and Angerami, 1968]. They showed that the spectral shape (dispersion) of whistlers arising from lightning strokes changed more or less discretely with satellite position, in a manner consistent with the traverse of separate whistler ducts. They determined that the equatorial separation of the ducts near $L = 3$ ranged from 50 to 500 km and that the equatorial thicknesses were about 400 km. Angerami [1970], using whistler dispersion data collected by the OGO 3 satellite, obtained equatorial separations from 110 to 1140 km and thicknesses from 223 to 430 km. He also concluded that density enhancements in whistler ducts generally lie between 6 and 22% and rarely exceed 33%. Scarf and Chappell [1973] reported the first simultaneous observations of whistler-mode waves and ambient plasma density obtained from a measurement of the H^+ ions. They reported duct thicknesses ranging from 68 to 850 km and density enhancements ranging from 10 to 40%. Of the six ducts observed, five were density enhancements and one was a density trough. Carpenter et al. [1981] reported duct-like features (both troughs and crests) in International Sun-Earth Explorer (ISEE-1) SFR data with a spatial size of 0.1 to 0.2 R_E (Earth radii) between $L = 4$ and $L = 5$. The density enhancements were not more than about 30%.

Since ground-based measurements of whistler dispersion have been used extensively to determine the electron density in the plasmasphere, it is important to determine whether waves propagate primarily within the enhancements, in troughs, or along density gradients. It is also important to determine the normal and extreme ranges for the density enhancements. Herein I report simultaneous satellite measurements of electron density and whistler-mode wave intensity with significantly higher time resolution than previous observations. These data show that the wave intensity is highest near the center of a plasma density enhancement and that the amplitude of the density enhancements can be significantly larger than previously reported.

II. DISCUSSION

A. INSTRUMENTATION

The data presented herein were obtained by the VLF/MF swept frequency receiver (SFR) aboard the AMPTE-IRM spacecraft. The scientific instrumentation aboard the spacecraft is described by Bryant et al. [1985]. The SFR is one component of the plasma wave experiment aboard the IRM. For a complete description of the instrument see Häusler et al. [1985]. The electric antenna is an extendable beryllium-copper dipole with a tip-to-tip length of 47.5 m. The nominal diameter is 5 mm. The antenna is covered with an insulating layer out to a distance of 15.55 m on each half of the dipole. The SFR covered the frequency range from 275 Hz to 99 kHz. The receiver has three separate 32-step spectrum analyzers. It produces a spectrum over linear frequency ranges from 275 to 2525 Hz every 2 s, and from 0.9 to 9 kHz and 9 to 99 kHz every 1 s. The bandwidth of the lower frequency spectrum analyzer is 100 Hz, the bandwidth of the middle frequency analyzer is 300 Hz, and the bandwidth of the higher frequency analyzer is 3000 Hz. The sweep in each channel is linear in frequency with time.

B. DENSITY MEASUREMENTS

Two radio techniques for measuring plasma density have been used here. Intense noise bands inside the plasmasphere have been associated with the upper hybrid resonance frequency by Mosier et al. [1973]. They show that the noise is generated between the plasma frequency and the upper hybrid resonance frequency. This provides an accurate determination of the electron density. Outside of the plasmasphere Gurnett and Shaw [1973] have identified a noise band known as continuum radiation. This is electromagnetic radiation with a sharply defined lower cutoff frequency at the local electron plasma frequency.

An outstanding example of plasma density enhancements was observed from 0300 to 0330 UT on January 12, 1986. The spectrogram in Fig. 1 shows the data from the SFR for that time period. The top panel, covering the frequency range from 9 to 99 kHz, shows an example of the noise band associated with the

upper hybrid resonance frequency. A second example was observed from 1100 to 1130 UT on September 23, 1985. The spectrogram in the top panel of Fig. 2 shows an example of continuum radiation extending above the local plasma frequency. In both cases we have found that the most intense part of the noise band is at its lower frequency end. We identify the plasma frequency with the channel containing this maximum signal.

An automatic data processing algorithm is used to select the channel with the maximum signal. A plot of the frequency vs time for this maximum channel is then compared with the color spectrogram. Occasionally, extraneous points occur due to electron cyclotron harmonic emissions at the low frequency end of the upper channel. The minimum allowable plasma frequency is raised until the extraneous points are eliminated.

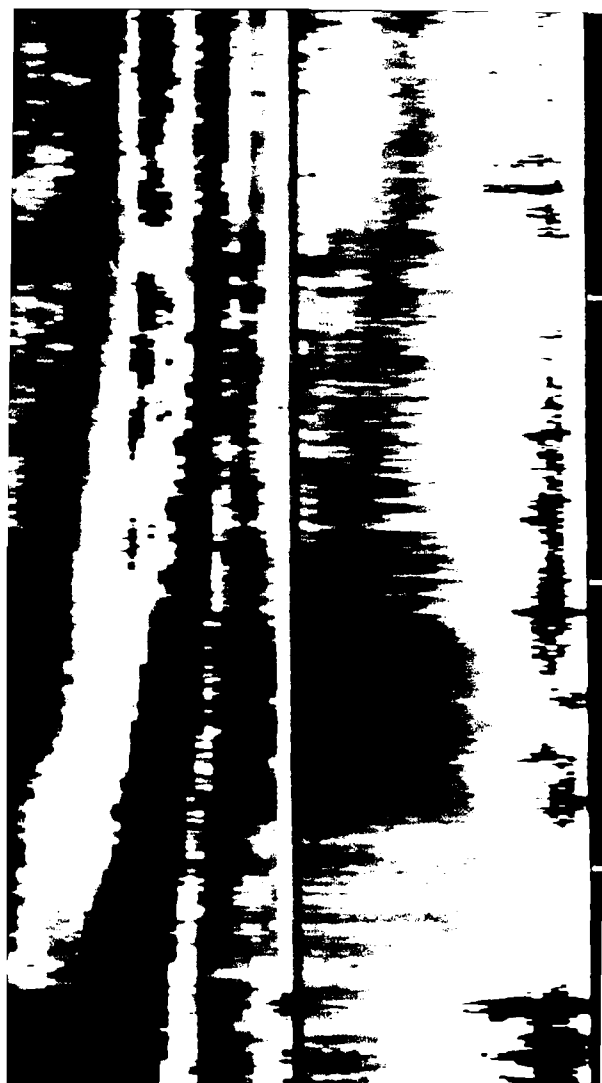
The upper frequency of the receiver, 99 kHz, sets the upper limit on the electron density, 100 cm^{-3} , that can be measured by the SFR. This restricts the density measurements to the outer plasmasphere in the vicinity of the plasmopause and to the outer magnetosphere. For this report the data survey was limited to the outer plasmasphere.

C. DATA

A total of 19 1-h spectrograms of the wave data were found covering the appropriate L-value range. Six were discarded because the identification of the location of the vehicle with respect to the plasmasphere was ambiguous.

Five cases occurred within the plasmasphere in the evening sector where the density gradient is small, L^{-3} , and the plasmopause is not well defined. Of these five, one had no density enhancements, two had well-defined density enhancements, and two had small density enhancements. All four with enhancements showed some correlation between the density enhancements and the waves.

Eight cases occurred away from the dusk sector where a density decrease could be identified with the plasmopause. In all but one of these cases, plasmaspheric hiss was present inside of the feature identified as the plasmopause. Of these eight cases, four had well developed ducts containing whistler-mode hiss. The remaining four had density enhancements but no correlated wave activity.



Generally, away from the dusk sector the outer region of the plasmasphere has density structures ranging from the extreme case observed on January 12, 1986, and described below, to much smaller structures observed on April 6, 1986. The largest structures on that day had half widths of 60 km and amplitudes of 50%. The full width from trough to trough was traversed by the AMPTE-IRM in 36 s. These structures would not have been resolved by the ISEE-1 SFR which sampled the complete spectrum in 32 s [Carpenter et al. 1981].

The following three cases exemplify well-defined structures with correlated whistler-mode waves.

1. CASE 1.

Figure 3a shows the electron density as a function of time obtained by applying the automatic data processing algorithm to the data in the top panel of Fig. 1 from 0300 to 0320 on January 12, 1986. Several large density enhancements can be seen in the data. During this time interval the spacecraft was outward bound from 4.9 to 5.5 R_E near 0345 local time. We interpret the final drop in frequency at 0325 UT in Fig. 1 to be the plasmopause. Then the density structures shown in Fig. 3a are all within the plasmasphere.

These measurements were made during a very quiet time period. At the time of the observations Kp was 1. For the preceding day the sum of Kp was 8-. The last time that Kp exceeded 2+ was 48 h before the observations.

Relatively intense signals can be seen extending upward in frequency to approximately 1500 Hz inside of the plasmasphere in Fig. 1. The frequency range and relatively constant amplitude over tens of seconds serve to identify them as hiss emissions. There is also a band of chorus emissions centered at 1800 Hz, beginning at 0320 UT and decreasing in frequency until they disappear at 0350 UT.

For the purpose of comparing the emissions with the density structures, we have chosen to use the signals in the 350 Hz frequency step of the low-frequency SFR. Figure 3b shows the amplitude of the waves at this frequency during the time period of the density measurements in Fig. 3a. The wave

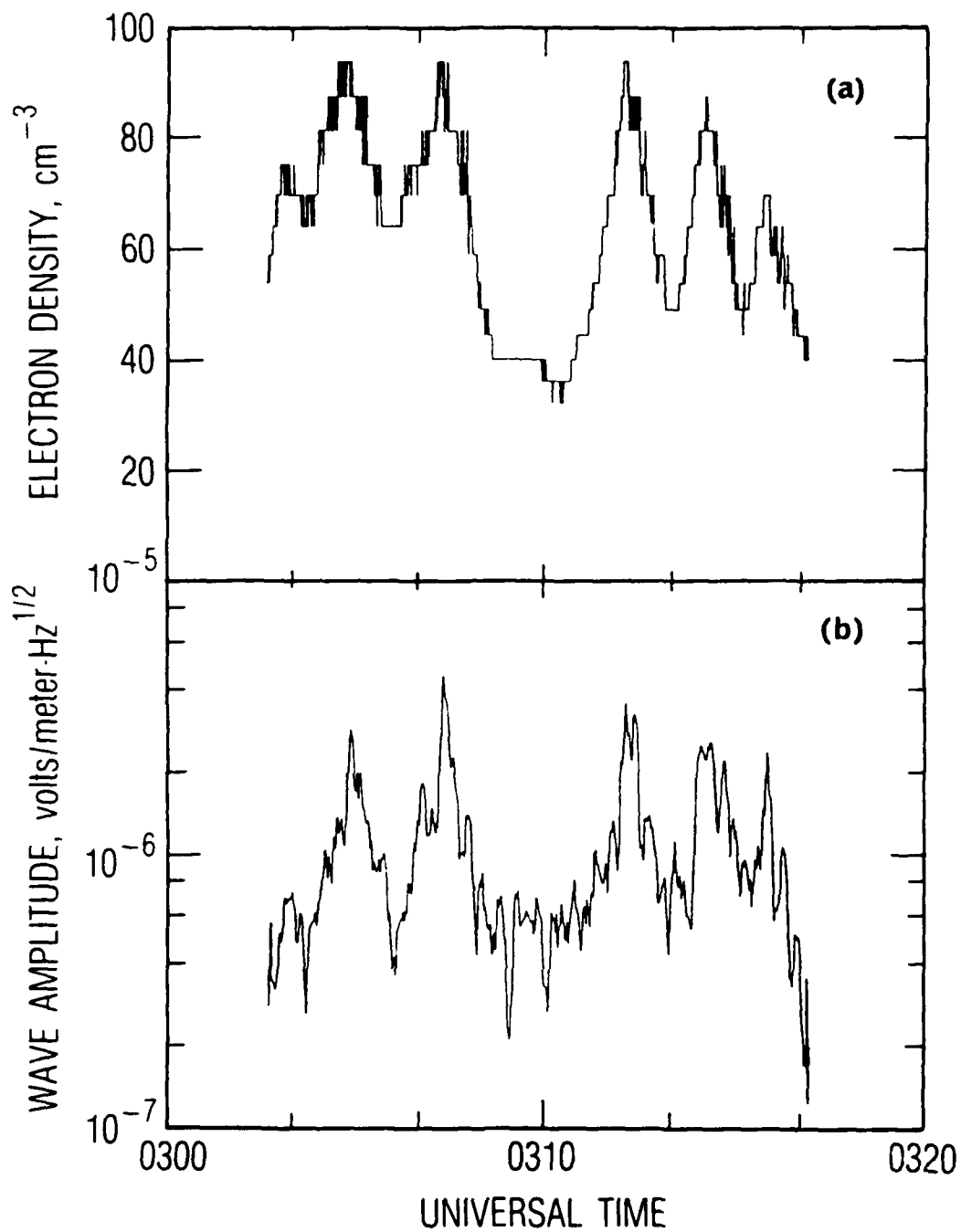


Fig. 3. (a) Electron Density and (b) Whistler-Mode Wave Amplitude at 350 Hz on January 12, 1986.

measurements have been smoothed by taking 10-s averages. The wave amplitude increases almost an order of magnitude from 4×10^{-7} to 4×10^{-6} V/m-Hz^{1/2} within each density enhancement.

A sample cross-correlation function of the density data in Fig. 3a and the wave data in Fig. 3b was calculated in order to determine the degree of correlation between the density enhancements and the wave enhancements. The resulting normalized cross-correlogram is shown in Fig. 4a. One lag period corresponds to 1 s. There is a well-defined peak corresponding to a correlation coefficient of approximately 0.5 near zero lag. This demonstrates that the waves are primarily contained within the density enhancements. We then interpret these density enhancements to be whistler-mode wave ducts.

The peak in the cross-correlogram actually occurs at a positive lag of 5 s. This sense of the lag is such that the wave maximum occurs at a slightly higher altitude than the density maximum. The radial velocity of the spacecraft is approximately 3.6 km/s during this time period. The offset between the wave maximum and the density maximum is thus about 18 km.

Table 1 contains a list of the percentage changes in density from trough to peak (positive) and from peak to trough (negative) for the ducts in Fig. 3a. For the well-defined density enhancements, the density changes range from 15 to 190%. Most of the ducts correspond to density enhancements near 50%. This is larger than previously reported [Smith and Angerami, 1968; Angerami, 1970; Scarf and Chappell, 1973; Carpenter et al., 1981]. The half-width of the ducts and the density gradients on each side of the ducts are also given in Table 1. The five best defined ducts in Fig. 3 have thicknesses ranging from 363 to 627 km. This agrees with previous measurements.

2. CASE 2.

The spectrogram in Fig. 2 from September 23, 1985, shows a more gradual decrease in the plasma frequency, and therefore the plasma density, with radial distance with no obvious steep density gradient signifying a plasma-pause. During this time interval the spacecraft was outward bound from 4.9 to 6.8 R_E near 1100 local time. The density profile obtained from Fig. 2 is

Table 1. Duct Parameters for the Density Enhancements Observed on January 12, 1986. The two columns for the percent density change are for the positive and negative slopes of the enhancement. The gradient is taken from the outer side of each duct.

Time (UT)	Density Change (percent)		Width (km)	Gradient (elec/cm ⁻³ -km)
	Pos.	Neg.		
0303:01	40	15	227	-0.08
0304:41	46	32	475	-0.12
0307:13	46	57	594	-0.18
0309:48	0	66	490	-0.06
0312:04	190	48	457	-0.17
0314:11	78	49	403	-0.21
0315:43	57	42	363	-0.12

shown in Fig. 5a. Here the minimum frequency used in the plasma frequency determination algorithm had to be raised to about 20 kHz to eliminate the strong electron cyclotron harmonic emissions below 20 kHz starting at 1105 UT. At the time of these observations $K_p = 4-$. During the preceding 24 h, K_p ranged from 1+ to 3+.

As on January 12, 1986, relatively intense signals can again be seen extending upward to 1500 Hz. On September 23, 1985, they appear across the entire spectrogram in Fig. 2. It is more difficult to classify the emissions in Fig. 2. Prior to 1115 UT they are most likely hiss emissions. After 1115 UT they may be a combination of hiss and chorus emissions.

The data from the 350 Hz step of the low frequency channel are shown in Fig. 5b. The cross-correlogram of the density and wave data is shown in Fig. 4b.

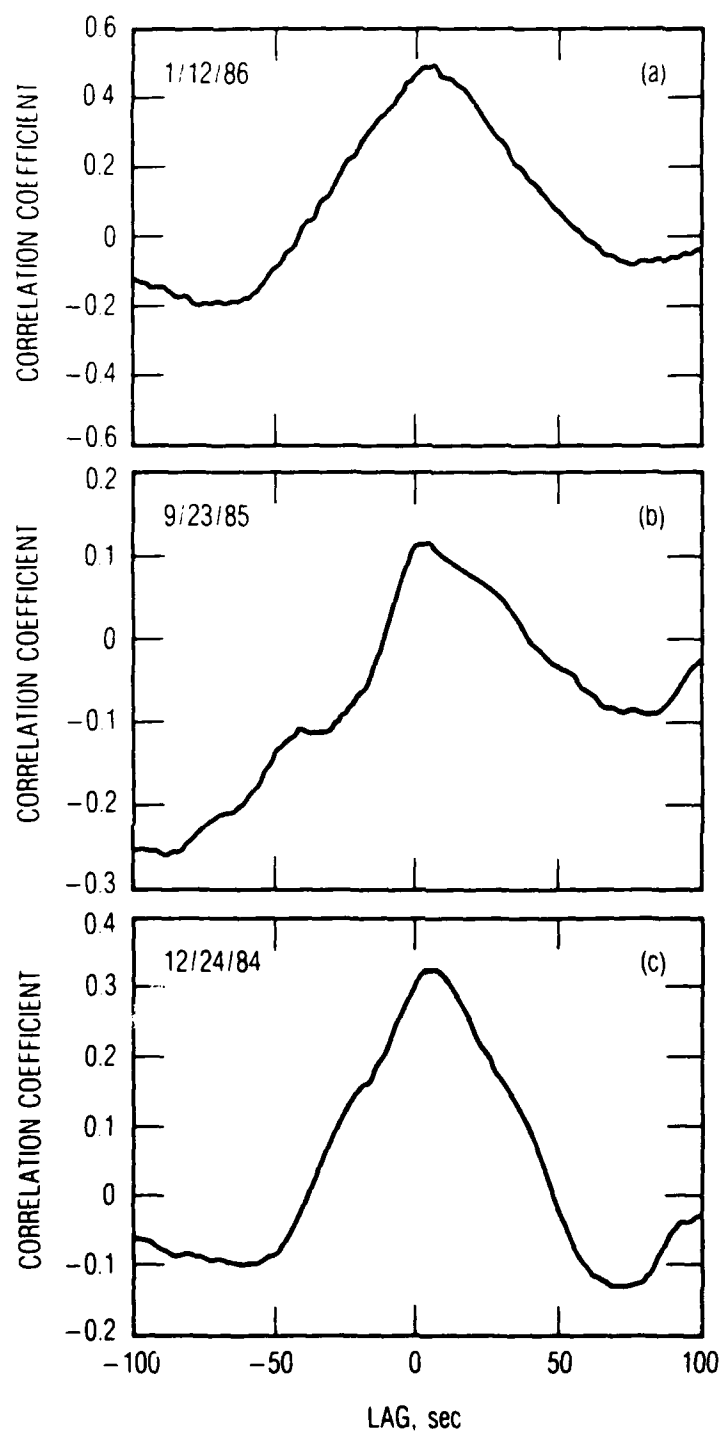


Fig. 4. Cross-Correlogram of the Electron Density and Whistler-Mode Wave Amplitude. (a) January 12, 1986; (b) September 23, 1985; (c) December 24, 1984.

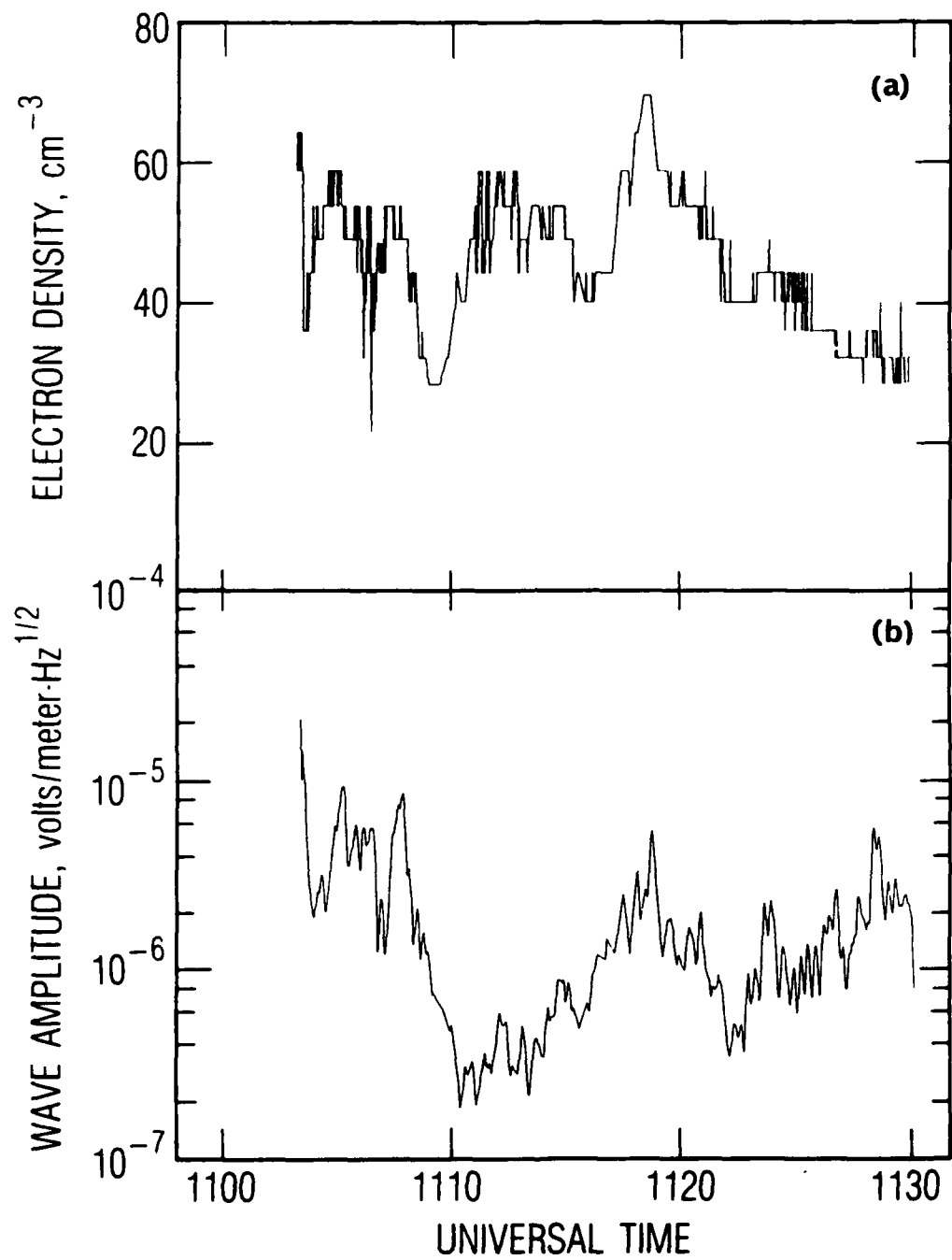


Fig. 5. (a) Electron Density and (b) Whistler-Mode Wave Amplitude at 350 Hz on September 23, 1985.

3. CASE 3.

At 1230 UT on December 24, 1984, plasma ducts were encountered on an outbound pass from 5.8 to 6.3 R_E . The plasma density and whistler-mode emissions at 350 Hz for this time period are shown in Figs. 6a and b, respectively. At the end of the time period shown in the figure, there is essentially no wave activity associated with the abrupt drop in density from 20 to 5 cm^{-3} . The value of Kp at the time of the observation was 1-. For the preceding 24 h, Kp ranged from 1- to 4-.

The normalized cross-correlogram of the density and wave data is shown in Fig. 4c. One lag period corresponds to 1 s. There is a well-defined peak corresponding to a correlation coefficient of approximately 0.35 near zero lag. The peak in the cross-correlogram is narrower than the peak for the data on January 12, 1986, shown in Fig. 4a. The peak is again offset from zero with a positive lag of 5 s, signifying that the wave maximum occurs at a slightly higher altitude than the density maximum. The radial velocity of the spacecraft is approximately 2.9 km/s during this time period. The offset between the wave maximum and the density maximum is thus about 15 km.

D. WHISTLER DUCTING CRITERION

Booker [1962] has applied waveguide mode theory to determine the minimum density enhancements necessary to produce ducting in a dipole geometry. In essence the criterion is that the curvature of the whistler-wave ray path must be equal to the curvature of the magnetic field line. For the plasma parameters pertinent to the case on January 12, 1986, we estimate the ratio of the ray path curvature to the field line curvature to be 12. This implies that the density enhancements are very effective wave ducts.

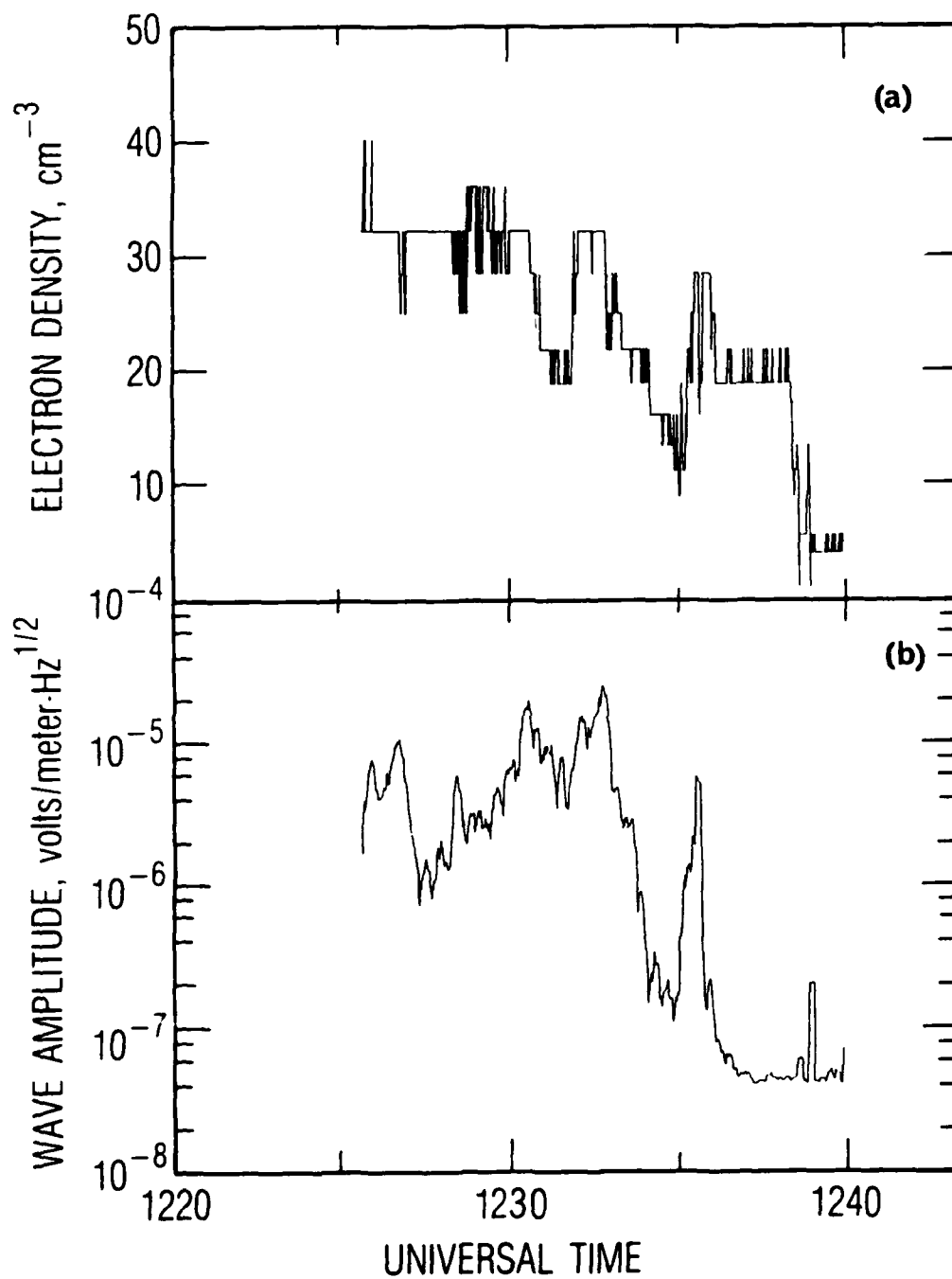


Fig. 6. (a) Electron Density and (b) Whistler-Mode Wave Amplitude at 350 Hz on December 24, 1984.

III. SUMMARY

Large density enhancements have been observed by the AMPTE-IRM spacecraft in the outer plasmasphere. The enhancements are comparable in radial dimension to previously reported whistler-mode wave ducts. However, the density enhancements are significantly larger than previously reported.

Whistler-mode emissions near the center of the ducts are typically an order of magnitude larger than emissions between the ducts. The emissions tend to reach their maximum intensity at a radial distance from the Earth that is slightly larger than the distance to the center of the duct.

REFERENCES

- Angerami, J. J., Whistler duct properties deduced from VLF observations made with the OGO 3 satellite near the magnetic equator, J. Geophys. Res., 75, 6115, 1970.
- Bryant, D. A., S. M. Krimigis, and G. Haerendel, Outline of the active magnetospheric particle tracer explorers (AMPTE) mission, IEEE Trans. Geoscience and Remote Sensing, GE-23, 177, 1985.
- Booker, H. G., Guidance of radio and hydromagnetic waves in the magnetosphere, J. Geophys. Res., 67, 4135, 1962.
- Carpenter, D. L., R. R. Anderson, T. F. Bell, and T. R. Miller, A comparison of equatorial electron densities measured by whistlers and by a satellite radio technique, Geophys. Res. Letters, 8, 1107, 1981.
- Gorney, D. J., and R. M. Thorne, A comparative ray-trace study of whistler ducting processes in the earth's plasmasphere, Geophys. Res. Letters, 7, 133, 1980.
- Gurnett, D. A., and R. R. Shaw, Electromagnetic radiation trapped in the magnetosphere above the plasma frequency, J. Geophys. Res., 78, 8136, 1973.
- Häusler, R., R. R. Anderson, D. A. Gurnett, H. C. Koons, R. H. Holzworth, O. H. Bauer, R. Treumann, K. Gnaiger, D. Odem, W. B. Harbridge, and F. Eberl, The plasma wave instrument onboard the AMPTE-IRM satellite, IEEE Trans. Geoscience and Remote Sensing, GE-23, 267, 1985.
- Inan, U. S., and T. F. Bell, The plasmopause as a VLF wave guide, J. Geophys. Res., 82, 2819, 1977.
- Mosier, S. R., M. L. Kaiser, and L. W. Brown, Observations of noise bands associated with the upper hybrid resonance by Imp 6 radio astronomy experiment, J. Geophys. Res., 78, 1673, 1973.
- Scarf, F. L., and C. R. Chappell, An association of magnetospheric whistler dispersion characteristics with changes in local plasma density, J. Geophys. Res., 78, 1597, 1973.
- Smith, R. L., Propagation characteristics of whistlers trapped in field-aligned columns of enhanced ionization, J. Geophys. Res., 66, 3699, 1961.
- Smith, R. L., and J. J. Angerami, Magnetospheric properties deduced from OGO 1 observations of ducted and nonducted whistlers, J. Geophys. Res., 73, 1, 1968.

LABORATORY OPERATIONS

The Aerospace Corporation functions as an "architect-engineer" for national security projects, specializing in advanced military space systems. Providing research support, the corporation's Laboratory Operations conducts experimental and theoretical investigations that focus on the application of scientific and technical advances to such systems. Vital to the success of these investigations is the technical staff's wide-ranging expertise and its ability to stay current with new developments. This expertise is enhanced by a research program aimed at dealing with the many problems associated with rapidly evolving space systems. Contributing their capabilities to the research effort are these individual laboratories:

Aerophysics Laboratory: Launch vehicle and reentry fluid mechanics, heat transfer and flight dynamics; chemical and electric propulsion, propellant chemistry, chemical dynamics, environmental chemistry, trace detection; spacecraft structural mechanics, contamination, thermal and structural control; high temperature thermomechanics, gas kinetics and radiation; cw and pulsed chemical and excimer laser development, including chemical kinetics, spectroscopy, optical resonators, beam control, atmospheric propagation, laser effects and countermeasures.

Chemistry and Physics Laboratory: Atmospheric chemical reactions, atmospheric optics, light scattering, state-specific chemical reactions and radiative signatures of missile plumes, sensor out-of-field-of-view rejection, applied laser spectroscopy, laser chemistry, laser optoelectronics, solar cell physics, battery electrochemistry, space vacuum and radiation effects on materials, lubrication and surface phenomena, thermionic emission, photosensitive materials and detectors, atomic frequency standards, and environmental chemistry.

Electronics Research Laboratory: Microelectronics, solid-state device physics, compound semiconductors, radiation hardening; electro-optics, quantum electronics, solid-state lasers, optical propagation and communications; microwave semiconductor devices, microwave/millimeter wave measurements, diagnostics and radiometry, microwave/millimeter wave thermionic devices; atomic time and frequency standards; antennas, rf systems, electromagnetic propagation phenomena, space communication systems.

Materials Sciences Laboratory: Development of new materials: metals, alloys, ceramics, polymers and their composites, and new forms of carbon; nondestructive evaluation, component failure analysis and reliability; fracture mechanics and stress corrosion; analysis and evaluation of materials at cryogenic and elevated temperatures as well as in space and enemy-induced environments.

Space Sciences Laboratory: Magnetospheric, auroral and cosmic ray physics, wave-particle interactions, magnetospheric plasma waves; atmospheric and ionospheric physics, density and composition of the upper atmosphere, remote sensing using atmospheric radiation; solar physics, infrared astronomy, infrared signature analysis; effects of solar activity, magnetic storms and nuclear explosions on the earth's atmosphere, ionosphere and magnetosphere; effects of electromagnetic and particulate radiations on space systems; space instrumentation.